Supporting Information for

Assembling Graphene Quantum Dots on Aminophenol-formaldehyde Resin towards Efficient Artificial Photocatalytic Hydrogen Peroxide Synthesis

Yuanjie Peng[a‡], Jiahong Lin[a‡], Jiewei Xiao[a], Xincheng Xie[b], Wenjie Yu[b], Hao Yan[a], Dongting Yue[a]*

a School of Environmental and Chemical Engineering, Shanghai University, NO.99 Shangda Road, Baoshan District, Shanghai 200444, P. R. China.

b National Facility for Protein Science in Shanghai, Shanghai Advanced Research Institute, Chinese Academy of Sciences, No. 99, Haike Road, Zhangjiang Hi-Tech Park, Pudong Shanghai, 201210, P.R. China.

Experimental Procedures

Chemicals and Regents

3-Aminophenol ($C_7H_9NO_2$, ≥ 99.0 wt %), citric Acid($C_6H_8O_7$, ≥ 99.0 wt %), formaldehyde (CH_2O, 37 wt % in water), ammonia ($NH_3·H_2O$, 25-28 wt % NH_3 in H_2O), sodium iodate ($NaIO_3$, ≥ 99.0 wt %), benzyl alcohol (C_7H_8O, 99%), cerium(IV) sulfate ($Ce(SO_4)_2$, ≥ 99.0 wt %), sulfuric Acid (95-98 wt %), deionized (DI) water with a resistivity of 18.2 MΩ·cm^{-1} at 25 ℃ was used in this study. All the aqueous solutions were prepared by using distilled and deionized water.

Preparation of APF and APF-GQDs-x

3-Aminophenol (110.0 mg, 1.0 mmol) was added into DI water (100 ml). After stirring continuously for 5 min, formaldehyde (37 wt % solution, 150 μl, 2.0 mmol) and $NH_3·H_2O$ (25~28 wt %, 100 μl, 0.4 mmol) were added and stirred at room temperature for 60 min. Then, a certain amount of quantum dot solution was added, and stirring continued for 5 hours to obtain APF-GQDs-x. The powers were washed thoroughly with DI water and collected by centrifuging, followed by overnight drying at room temperature under a vacuum.

Photocatalyst characterizations

The synthesized samples underwent thorough structural and morphological analysis using various techniques. X-ray powder diffraction (XRD) was employed to examine the structure, utilizing a Rigaku D/max 2500 powder diffractometer with Cu Kα radiation. The morphology was further investigated through transmission electron microscopy (TEM) using a JEM-F200 model and scanning electron microscopy (SEM) with a Gemini G300. Surface elemental composition was determined via X-ray photoelectron spectroscopy (XPS) conducted on a Thermo Scientific K-Alpha$^+$ system, employing specific instrument conditions including Al K Alpha as the source gun type, ion energy of 1486.6 eV, and a beam spot of 400μm, among others. Peak fitting was accomplished using mixed Gaussian/Lorentzian peak shapes after subtraction of Shirley's background. Furthermore, electron paramagnetic resonance (EPR) spectra

obtained from a Bruker Emxplus instrument were utilized to investigate reactive radicals generated during the activation of H_2O_2. These radicals were captured by the spin-trapping agent 5,5-dimethylpyrroline-oxide (DMPO), with a center field at 3350 G, providing valuable insights into the activation process. The absorption spectra for the polymers were recorded on a Shimadzu UV-3600i Plus as powders. Detailed band structures were analyzed by using ultraviolet photoelectron spectroscopy (UPS) with a PHI5000 Versaprobe III (Scanning ESCA Microprobe) SCA (Spherical Analyzer). Photoluminescence (PL) spectra of the synthesized polymers were characterized by the Horiba FluoroLog-QM spectrofluorometer with a CW diode laser (980 nm). The fluorescence lifetime was recorded on a Horiba Fluorolog-QM steady-state and time-resolved fluorescence spectrometer. Electron paramagnetic resonance (EPR) spectra from a Bruker Emxplus were used to probe the reactive radicals generated during activation of H_2O_2, captured by spin trapping agent 5,5-dimethylpyrroline-oxide (DMPO) and 2,2,6,6-Tetramethylpiperidine-1-oxyl (TEMPO) with a center field at 3350 G.

Photoelectrochemical measurement

The cyclic voltammetry (CV) was performed on the Zennium electrochemical workstation (Zahner) with a three-electrode system, where an L-type glassy carbon electrode (L-GCE) as the working electrode, a Pt wire as the counter electrode, an Ag/AgCl electrode (3 M KCl) as the reference electrode. The GCE was cleaned before each run by polishing with 0.3 mm and 0.05 mm alumina slurry and then rinsing with ultrapure water. Electrochemical impendence spectra (EIS) were performed on the Zennium electrochemical workstation (Zahner) with a three-electrode system, where a Pt foil and Ag/AgCl electrode were used as the counter and reference electrodes, respectively. A 150W–Xenon lamp (CEL–S500, CEAULIGHT) was used as the light source. The CV and EIS tests were performed under continuous O_2 bubbling at different temperatures.

The preparation method of the working electrodes is as follows. The catalyst ink was prepared by mixing 3 mg of catalyst, 0.1 mL of DI water, 0.05 mL of 0.5% Nafion, and 1.80 mL of EtOH and ultra-sonicating for at least 30 min. Next, 10 µL of the ink was

dropped on the polished L-GCE. Finally, the as-prepared catalyst film was dried at room temperature.

Photocatalytic H_2O_2 production

Briefly, 5.0 mg catalyst and 50.0 mL H_2O were added to the 300.0 mL reactor with continuous O_2 bubbling. The bottle was photoirradiated by AM1.5G simulated sunlight irradiation using a 150W–Xenon lamp (CEL–S500, CEAULIGHT), and the reactions were performed at room temperature. After the reactions, the solution was filtered through a 0.45-μm polytetrafluoroethylene (PTFE) filter to remove the catalyst, and the H_2O_2 amount was quantified by a traditional cerium sulfate $Ce(SO_4)_2$ titration method[1]. For the determination of SCC efficiency, an AM1.5G solar simulator was used with 1.0 g of catalyst and 200.0 ml of water under O_2 bubbling (0.1 min^{-1}) at 303K. The SCC efficiency was determined using.

$$\text{SCC efficiency (\%)} = \frac{\Delta G\ For\ H_2O_2\ generation\ (J/mol)\ \times\ Formed\ H_2O_2\ (mol)}{Unit\ input\ energy\ (W/cm2)\ \times\ The\ irradiated\ area\ (cm2)\ \times\ Reaction\ time\ (s)} \times 100\%$$

ΔG–The free energy of H_2O_2 production is 117 kJ/mol.

Unit input power (W/cm^2) –The radiation intensity of the light source is 0.1W/cm^2 with an AM1.5 global filter for 300 ~ 2500 nm.

The irradiated area (cm^2) –1.0×1.0 cm^2.

Reaction time–3600 s.

The amount of H_2O_2 generation is 35.1 μmol.

$$SCC\ efficiency\ (\%) = \frac{117000\ (J/mol) \times 35.1 \times 10^{-6}\ (mol)}{0.1\ (W/cm^2) \times 1.0\ (cm^2) \times 3600(s)} \times 100\% = 1.14\%$$

For AQE measurements, 1.0 g of photocatalyst was dispersed in 200.0 mL H_2O. A 150 W Xe-lamp with a band-pass filter of 420 nm was used as the incident light source. The irradiation area was controlled to be 1.0 cm^2. The amount of H_2O_2 production was analyzed after 1 h irradiation. AQE was calculated using the following equation:

$AQE\% = 2 \times (N_{H_2O_2} N_A \cdot h \cdot c) / (I \cdot S \cdot t \cdot) \times 100\%$

where $N_{H_2O_2}$ was the amount of H_2O_2 production (mol), N_A was the Avogadro constant (6.022×10^{23} mol^{-1}), h was the Planck constant (6.626×10^{-34} J·s), c was the

speed of light ($3x10^8$ $m \cdot s^{-1}$), I was the irradiation intensity ($W \cdot cm^2$), S was the irradiation area (cm^2), t was the irradiation time (s) and λ was the wavelength of incident light (nm).

Stability Test

50 mg catalyst and 50 mL H_2O were added to the 300 mL reactor with continuous O_2 bubbling at room temperature. The cycling photocatalytic test to investigate the photocatalytic stability was performed every 3 h as a cycle. The catalyst was recovered by centrifuging the sample.

Practical Application Test

The tap water, lake water from Panchi Lake in Shanghai University, and real seawater from the East China Sea were used for photosynthesis of H_2O_2 in ambient conditions. In detail, 5 mg catalyst and 50 mL solution were added to the 300 mL reactor and photothermal reactions were performed under continuous O_2 bubbling or open air at room temperature.

Isotope labeling experiments.

10 mL H_2O containing APF-GQDs (100 mg) was added into the closed glass tube. After vacuuming, the reactor was filled with Ar gas. Then $^{18}O_2$ was injected and the reactor was irradiated with a 150 W xenon lamp (AM 1.5G) for 24 hours. After the reaction, the remaining $^{18}O2$ gas was removed by vacuuming the reactor. Then MnO_2 aqueous solution (Ar saturation) was injected into the reactor to convert H_2O_2 into O_2, and the gas products were analyzed by gas chromatography-mass spectrometry (GC-MS, MAT-271).

Rotating disk electrode (RDE) measurements

The electrochemical ORR was measured on a CHI760E Electrochemical Workstation (CH Instruments) with a three-electrode configuration electrochemical cell. The graphite rod and Ag/AgCl electrode were chosen as the counter electrode and reference electrode, respectively. The rotating ring disk electrode with an electrode area of 0.2475 cm^2 (RRDE, PINE Research Instrumentation) was used as the working electrode. The catalyst ink was prepared by mixing 3 mg of catalyst, 0.1 mL of DI water, 0.05 mL of 0.5% Nafion, and 1.80 mL of EtOH and ultra-sonicating for at least

30 min. Next, 10 μL of the ink was dropped on the polished RRDE and dried at room temperature.

Before the ORR, the pre-activation process by scanning cycle voltammetry (CV) curves (20 cycles, scan rate: 50 mV/s) was performed on RRDE to electrochemically clean it until stable CV curves were obtained. The ORR polarization curves were assessed by linear sweep voltammograms (LSV) from 1.1 to 0.2 V (vs. RHE) with the sweep speed of 10 mV s^{-1} at 1600 rpm in O_2-saturated 0.1 M KOH (without iR correction), and Pt ring potential was maintained at 1.3 V (vs. RHE) to respond to the generated H_2O_2.

The H_2O_2 selectivity and the transfer number electron (n) were calculated based on the disk current and ring current data as the following formulas:

$$\lambda(H_2O_2, \%) = 200 * \frac{Iring/N}{Idisk + Iring/N}$$

$$n = 4 * \frac{Idisk}{Idisk + Iring/N}$$

In-situ Synchrotron Radiation-based Fourier Transform Infrared Microscopy (SR-FTIR) Measurement Method.

The measurements of SR-FTIR including infrared microspectroscopic analysis, were performed at the BL01B beamline of the National Facility for Protein Science in Shanghai (NFPS) at Shanghai Synchrotron Radiation Facility (SSRF). All spectra were acquired in transmission mode on a Nicolet 6700 FTIR spectrometer coupled with a Nicolet Continuμm infrared microscope from ThermoFisher Scientific.

Supplementary Figures

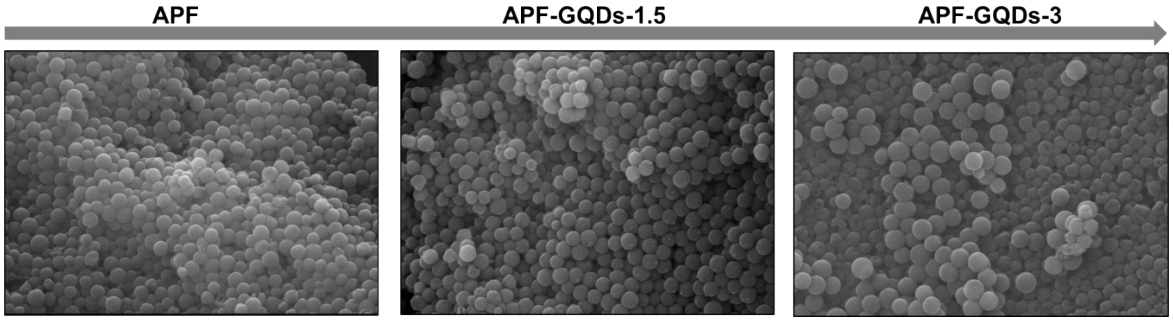

Fig. S1 SEM images of APF-GQDs-x.

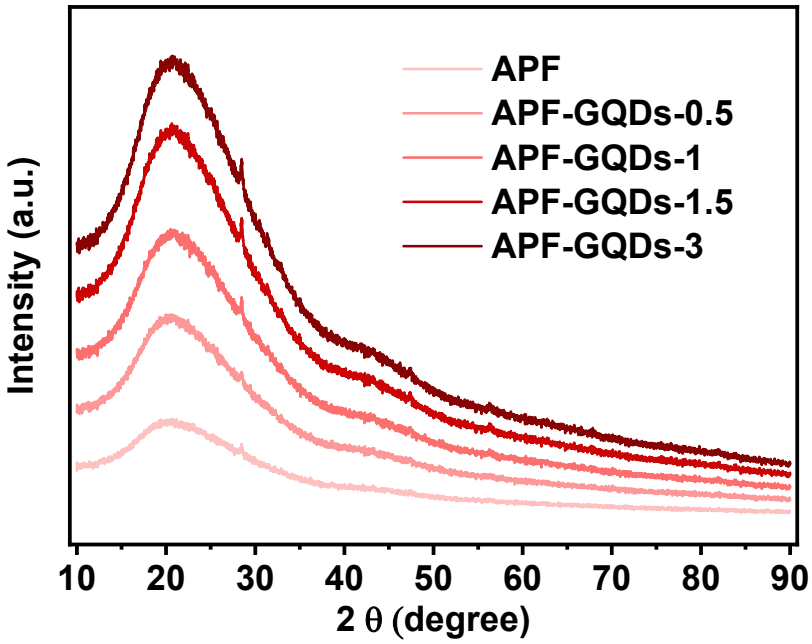

Fig. S2 XRD patterns of APF and APF-GQDs-x.

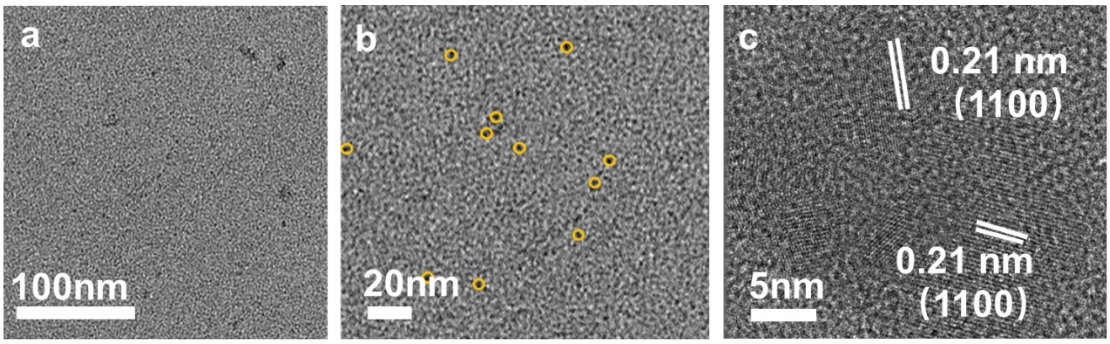

Fig. S3 TEM and HRTEM images of GQDs

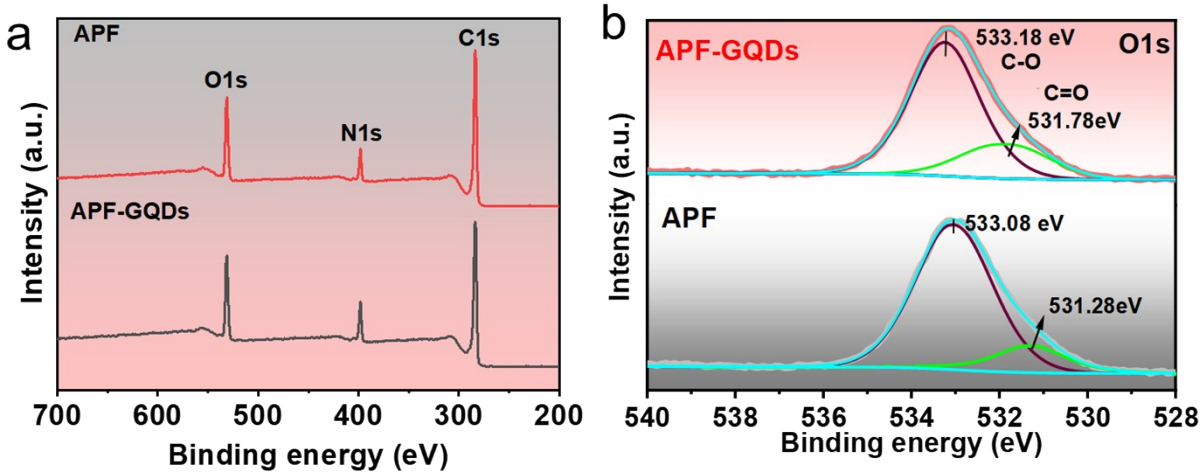

Fig. S4 (a) XPS survey and (b) O1s high-resolution XPS spectra of APF and APF-GQDs.

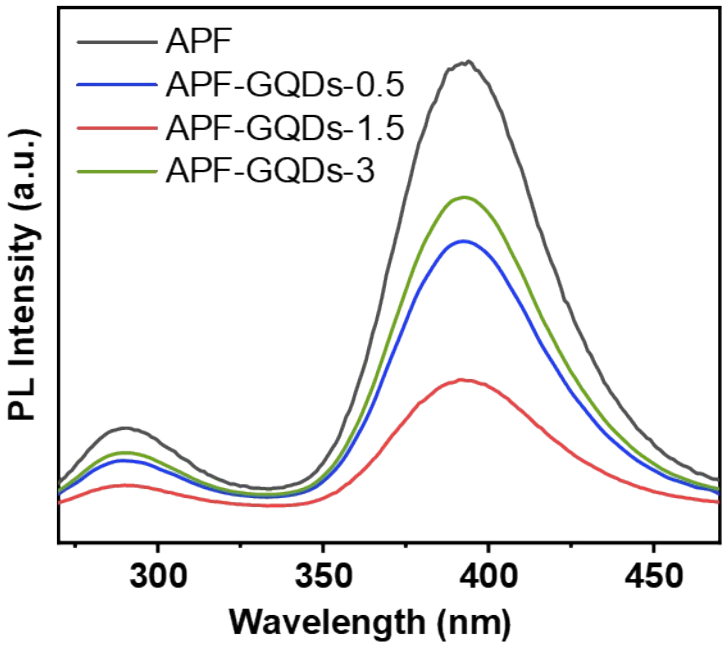

Fig. S5 Photoluminescence spectroscopy of APF and APF-GQDs.

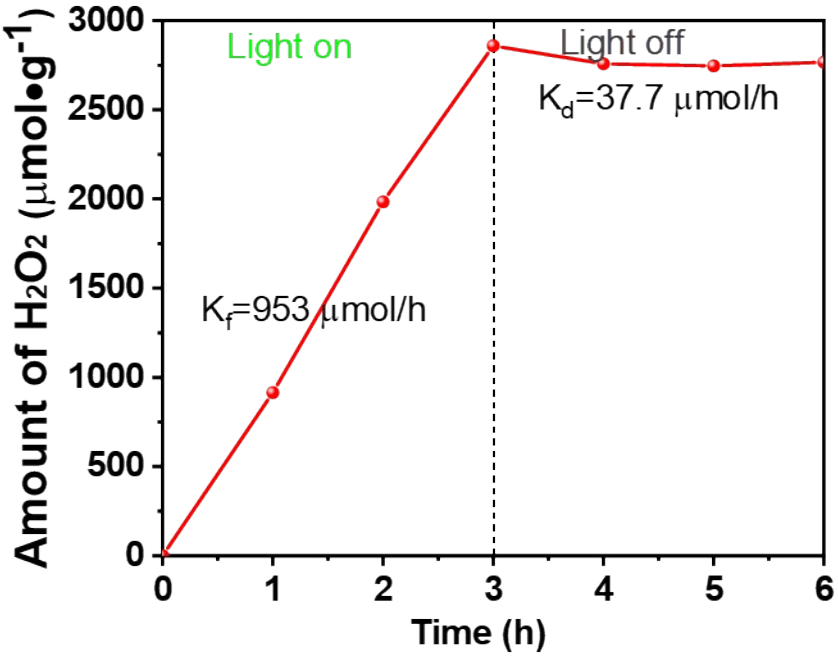

Fig. S6 The variation of photocatalytic hydrogen peroxide production over time under light and dark conditions.

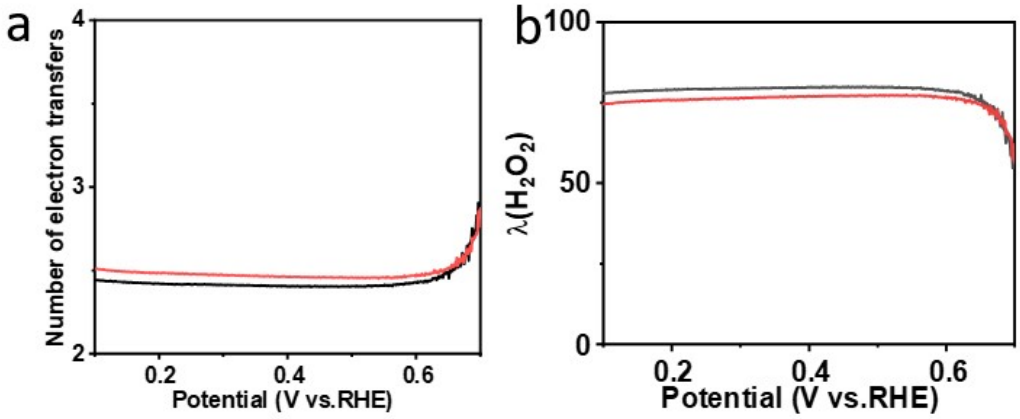

Fig. S7 (a) Electron transfer number (n) and (b) H_2O_2 selectivity of APF (black curve) and APF-GQD (red curve).

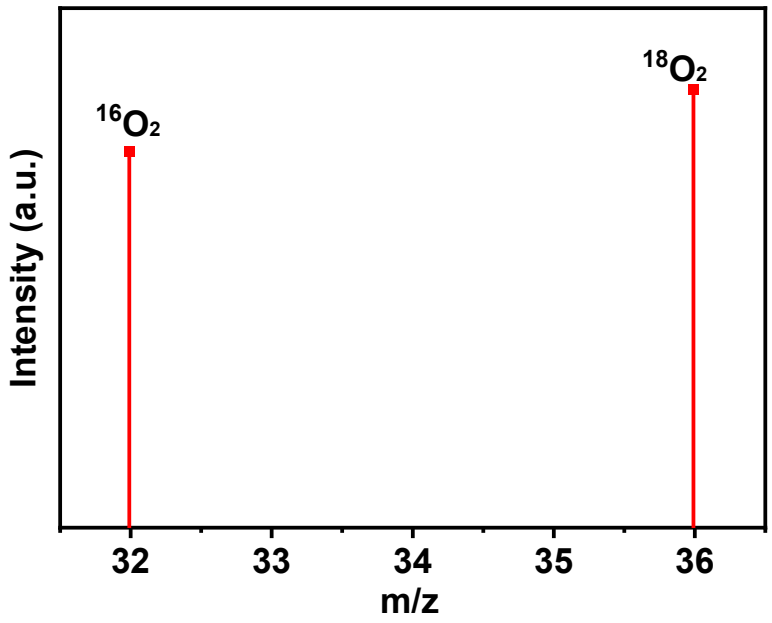

Fig.S8 GC-MS charts for O_2 evolved by decomposition of H_2O_2 produced by isotopic photoreaction experiments.

Table S1. Elemental content of pristine APF and APF-GQD.

Samples	C(%)	N(%)	O(%)
Pristine APF resin	73.48	10.59	15.93
APF-GQDS-1.5	74.54	11.46	14

Table S2. Summary of materials for photocatalytic H_2O_2 generation activity.

Catalyst	Atmosphere	Light Source	Amount of H_2O_2 ($\mu mol \cdot g^{-1} \cdot h^{-1}$)	SCC efficiency (%)	Ref.
In_2S_3-CQDs	O2	150W Xe lamp	634	0.16	[2]
QAP2	O2	300W Xe lamp (λ≥420nm)	380	---	[3]
CDs10MCN	O_2	300W Xe lamp (λ≥420nm)	423.17	---	[4]
MRF	O_2	300W Xe lamp (λ≥420nm)	575	0.84	[5]
Resin	O_2	300W Xe lamp (λ≥420nm)	82	0.8	[6]
MPaCOFs/CQDs-2	O_2	300W Xe lamp (λ≥420nm)	540	0.85	[7]
Nv-C≡N-CN	O_2	300W Xe lamp (λ≥420nm)	323	0.23	[8]
APF	O_2	150W AM 1.5G solar simulator	330.3	--	This work
APF-GQDs-1.5	O_2	150W AM 1.5G solar simulator	978	1.14	This work

1 Z. Lu, G. Chen, S. Siahrostami, Z. Chen, K. Liu, J. Xie, L. Liao, T. Wu, D. Lin, Y. Liu, T. F. Jaramillo, J. K. Nørskov and Y. Cui, *Nat. Catal.* 2018, **1**, 156-162.

2 A. Tikoo, A. K. S. Koushik and P. Meduri, *ACS Appl. Eng. Mater.* 2023, **1**, 1397-1407.

3 B. Sheng, Y. Xie, Q. Zhao, H. Sheng and J. Zhao, *Energy Environ. Sci.* 2023.

4 H. Guo, L. Zhou, K. Huang, Y. Li, W. Hou, H. Liao, C. Lian, S. Yang, D. Wu, Z. Lei, Z. Liu and L. Wang, *Adv. Funct. Mater.* **50**, 2402650.

5 L. Yuan, C. Zhang, J. Wang, C. Liu and C. Yu, *Nano Res0* 2021, **14**, 3267-3273.

6 Y. Shiraishi, T. Takii, T. Hagi, S. Mori, Y. Kofuji, Y. Kitagawa, S. Tanaka, S. Ichikawa and T. Hirai, *Nat. Mater.* 2019, **18**, 985-993.

7 Y. Zhao, Y. Liu, J. Cao, H. Wang, M. Shao, H. Huang, Y. Liu and Z. Kang, *Appl. Catal. B: Environ.* 2020, **278**, 119289.

8 X. Zhang, P. Ma, C. Wang, L. Gan, X. Chen, P. Zhang, Y. Wang, H. Li, L. Wang, X. Zhou and K. Zheng, *Energy Environ. Sci.* 2022, **15**, 830-842.